

Effects of orthodontic treatment on human alveolar bone density distribution

Hechang Huang · Michael Richards · Tamer Bedair ·
Henry W. Fields · J. Martin Palomo ·
William M. Johnston · Do-Gyoon Kim

Received: 30 March 2012 / Accepted: 4 December 2012 / Published online: 20 December 2012
© Springer-Verlag Berlin Heidelberg 2012

Abstract

Objectives The objective of this study was to examine if non-invasive clinical cone beam computed tomography (CBCT)-based degree of bone mineralization (DBM) measurement can be used to detect the different results from orthodontic treatment between the maxilla and mandible in human patients.

Materials and methods CBCT images were taken before and after orthodontic treatment from 43 patients (19 males and 24 females, 14.36 ± 1.50 years). A histogram of computed tomography (CT) attenuation value, which is equivalent to the DBM, was obtained from the alveolar cortical (AC), trabecular (AT), and enamel (E) regions of each image. Mean, standard deviation (SD), and coefficient of variation (COV) of the CT attenuation values were computed. The regional variations and percentage (%) differences between the E and alveolar regions of the CT attenuation

parameters at the maxilla and mandible were analyzed before and after orthodontic treatment.

Results The AC had higher mean and variability (SD and COV) than the AT before and after treatment ($p < 0.001$). The variability was higher in the mandibular AC than in the maxillary AC ($p < 0.01$) independent of orthodontic treatment. The percentage (%) difference of variability of CT attenuation values changed for both AT and AC in the maxilla after orthodontic treatment, while that changed for only the AT ($p < 0.02$), but not for AC, in the mandible ($p > 0.16$).

Conclusions The alveolar cortical region of the mandible responded differently to orthodontic treatment compared with other alveolar regions.

Clinical relevance The CBCT-based DBM analysis can be used clinically to assess alveolar bone quality changes induced by orthodontic treatment to improve treatment planning and result evaluation.

Keywords Orthodontic · Alveolar bone · Density · CBCT

H. Huang · M. Richards · H. W. Fields · D.-G. Kim (✉)
Division of Orthodontics, College of Dentistry, Ohio State
University, 305 W 12th Avenue,
Columbus, OH 43210, USA
e-mail: kim.2508@osu.edu

T. Bedair
Faculty of Dentistry, Suez Canal University, Ismailia, Egypt

T. Bedair
Umm Al-Qura University, Makkah, Kingdom of Saudi Arabia

J. M. Palomo
Department of Orthodontics, School of Dental Medicine,
Case Western Reserve University, 2124 Cornell Road,
Cleveland, OH 44106, USA

W. M. Johnston
Division of Restorative, Prosthetic and Primary Care Dentistry,
College of Dentistry, Ohio State University, 305 W 12th Avenue,
Columbus, OH 43210, USA

Introduction

Orthodontic tooth movement involves changes in the gingival [1], the periodontal ligament [2–7], and the alveolar bone [8–14]. Many studies have observed changes of alveolar bone density due to active bone remodeling during orthodontic treatment [12, 13, 15, 16]. These density alterations of alveolar region result from resorption of pre-existing bone tissue and formation of new bone tissue in the process of bone remodeling. As the new bone tissue has less mineral content than the pre-existing bone tissue, the distribution of the degree of bone mineralization (DBM) inherently changes [17, 18]. It was found that the DBM determines the mechanical response of bone tissue to the applied force [19, 20], and it is well known that mechanical

orthodontic force stimulates bone remodeling in the alveolar process [8, 10–14, 21]. Taken together, it is likely that the DBM distribution reflects bone response to orthodontic force at the initiation and progress of bone remodeling and also provides the status of bone alteration resulting from bone remodeling. However, not many studies have been done to examine the DBM distribution changes in human patients during orthodontic treatment.

The X-ray-based computed tomography (CT) images have been used to obtain detailed morphology and mineral density of the patient's jaw bone [15, 16, 22]. As cone beam computed tomography (CBCT) can provide three-dimensional images at the micron-level high resolution and has relatively lower radiation level compared with multislice CT (MSCT) [23–26], it has been widely used for diagnosis and treatment planning for the craniofacial region in clinic [22]. To date, most of the CBCT image-based studies have focused on morphological analysis because the CBCT-based mineral density measurement was not fully established. Although previous studies verified the applicability of CBCT attenuation value to assess the mineral content of the jaw bone [27, 28], it was indicated that the CT attenuation values varied by different scanning conditions [29, 30]. Currently, a new approach to compare the mineral densities between CBCT images is demanded.

It has been indicated that the alveolar bone remodeling process responding to orthodontic treatment is different between the maxilla and mandible and that the rate and type of tooth movement are affected by the level of alveolar bone remodeling [31]. These observations were obtained using histomorphological analyses of animal models to understand the mechanism of biological activities involved in

orthodontic tooth movement. However, the destructive histomorphological procedure limits the possibility to investigate the case of human patients. Thus, the objective of this study was to examine if non-invasive CBCT-based DBM measurement can be used to detect the different results from orthodontic treatment between the maxilla and mandible in human patients. An internal reference was also tested to compare the DBM measures using the CBCT images before and after orthodontic treatment.

Materials and methods

This research protocol was approved by the Institutional Review Board at The Ohio State University. CBCT images of 43 patients (19 males and 24 females, mean initial age of 14.36 ± 1.50 years old, range of 11.5 to 17.4 years) were randomly collected using retrospective records before and immediately after comprehensive orthodontic treatment with full fixed appliances (20.05 ± 4.18 months of treatment duration) at the Craniofacial Imaging Center at Case Western Reserve University School of Dental Medicine. The CBCT images were taken at a scanning condition (2 mA and 120 kV) with voxel size of 292 or 377 μm (Hitachi Medical Systems America Inc., Twinsburg, OH, USA) (Fig. 1). These images were from patients who did not have craniofacial anomalies, facial asymmetry, orthognathic surgery, rapid palatal expansion, head gear, or tooth extraction (except for the third molars) during orthodontic treatment. The commercial software (Microview 2.1.2, GE) was utilized to determine a global threshold CT value for each CBCT image. The algorithm of this software was originally

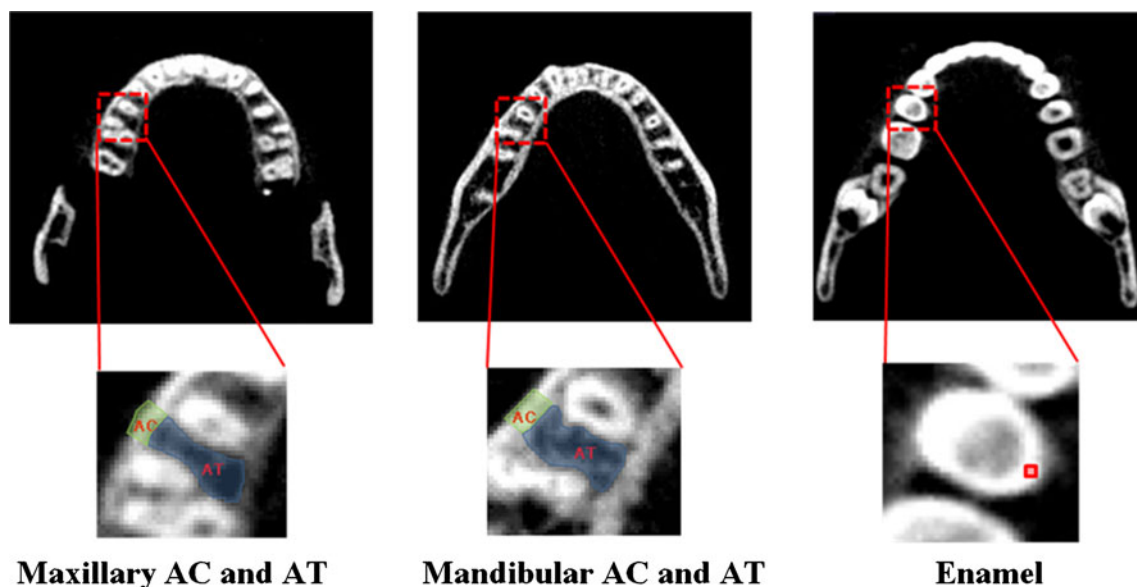


Fig. 1 Typical CBCT images with the locations of interest. *AT* alveolar trabecular bone (blue area), *AC* alveolar cortical bone (green area), and enamel (red square)

developed to segment bone voxels in a micro-CT image. It determines the global threshold value at a centerline between the maximum and minimum CT values of all bone and non-bone voxels in the region of interest similar to a previous study [32]. As a result, this approach provides a more conservative global threshold value than other algorithms, which can isolate the voxels with apparently higher CT values compared to neighbor voxels. The global threshold value of CT attenuation for each individual image was used to segment bone voxels from soft tissues and background noise and was maintained during segmentation to give a histogram of the CT values for each region of interest. ImageJ (NIH) software was used to analyze all the CBCT images.

In both maxilla and mandible, the region between the left second premolar (P2) and first molar (M1) inside the field of view was examined. For each sample, the middle axial slice between the tooth root tip of the P2 and the inter-dental alveolar crest between the P2 and the M1 was identified, together with two above and two below axial slices. Thus, five slices of images were used to visually identify and measure the alveolar trabecular region (AT) and buccal alveolar cortical region (AC) in the left maxilla and mandible (Fig. 1). An enamel region (E) located midway mesial-distally in the middle five axial slices between the left mandibular P2 lingual cusp tip and the cemento-enamel junction was identified. A fixed area (2×2 voxels) of enamel region was visually identified within each slice (Fig. 1). The name of each image was coded by assigning a random ID number, and the demographic and treatment information of the patients was concealed from the raters. The sequence of image analysis was randomized using the coded name of each image.

A histogram of the CT attenuation value (Hounsfield unit), which was equivalent to the DBM [28, 33], was analyzed. The CT attenuation parameters, mean, standard deviation (SD), and coefficient of variation ($COV = SD / \text{mean}$), were calculated based on the histogram of intra-specimen CT attenuation values measured from the five slices for each region in the same CBCT image. Percentage (%) differences of the mean, SD, and COV between each of the AT and AC with the E ($((AT-E)/(AT+E)/2) \times 100$) and ($((AC-E)/(AC+E)/2) \times 100$) in the same CBCT image were calculated to compare these relative values between the CBCT images before and after orthodontic treatment. All the measurements were performed by three raters (HH, MR, and TB) while blinded for the demographic information of patients using the randomly coded CBCT images. Repeated measurements for reliability tests (five samples each) were made at least 6 weeks since the original measurements. Intra- and inter-rater agreements were analyzed with intra-class correlation coefficient with Shrout–Fleiss random set method and single score method, respectively (SAS, Cary, NC, USA). Within each CBCT image, differences of the CT

attenuation values between alveolar regions (AT and AC) were tested using a repeated measures analysis of variances with Bonferroni correction and Tukey–Kramer tests before or after orthodontic treatment (SAS, Cary, NC, USA). The percentage differences of the CT attenuation parameters were compared between CBCT images before and after orthodontic treatment for the same patient using paired *t* test (Microsoft Excel). Significance was set at $p \leq 0.05$.

Results

The CT attenuation parameters (mean, SD, and COV) were successfully obtained from each CBCT image (Table 1). Inter-rater reliability among raters MR, HH, and TB was 0.97, 0.95, and 0.97 for mean, SD, and COV, respectively.

The regional variation of the CT attenuation parameters was compared for an individual CBCT image (Table 1). The means of all of the CT attenuation parameters were significantly lower in the AT region than in the AC region of the maxilla (Mx) and mandible (Md) both before and after orthodontic treatments ($p < 0.001$). Before orthodontic treatment, the means of all of the CT attenuation parameters of the alveolar trabecular region were not significantly different between the maxilla and the mandible ($p > 0.68$), while those of the alveolar cortical region were significantly lower in the maxilla than in the mandible ($p < 0.001$). After orthodontic treatment, the means of the mean and SD of the alveolar trabecular region and the mean of the alveolar cortical region were not significantly different between the maxilla and the mandible ($p > 0.16$), while the means of the COV of the alveolar trabecular region was higher in the maxilla than in the mandible ($p < 0.03$), and the means of the SD and COV of the alveolar cortical region were lower in the maxilla than in the mandible ($p < 0.01$).

The inter-regional percentage (%) differences of CT attenuation parameters between the alveolar regions (AT and AC) and the enamel region (E) were compared before and after orthodontic treatment (Fig. 2). In the maxilla (Fig. 2a, b), the means of the percentage differences of all of the CT attenuation parameters between the alveolar trabecular region and the enamel region (%AT-E) and between the alveolar cortical region and the enamel region (%AC-E) significantly increased after orthodontic treatment ($p < 0.02$ for both). In the mandible (Fig. 2c, d), the means of the percentage differences of the mean and SD between the alveolar trabecular region and the enamel region (%AT-E) and those of the mean between the alveolar cortical region and the enamel region (%AC-E) significantly increased after orthodontic treatment ($p < 0.01$ for both). The means of the percentage differences of other parameters between the alveolar regions and the enamel region did not change after orthodontic treatment ($p > 0.09$).

Table 1 CT attenuation parameters (mean, SD, and COV) obtained from five slices within each region before and after treatment

Structure	Before treatment			After treatment		
	Mean	SD	COV	Mean	SD	COV
Mx AT	966.59±106.78	86.00±28.61	0.089±0.027	1,060.95±66.01	88.49±25.24	0.083±0.022
Mx AC	1,096.24±129.56	121.20±43.43	0.111±0.037	1,189.27±94.89	134.50±31.90	0.114±0.028
Md AT	955.60±99.33	78.16±23.77	0.082±0.023	1,064.98±75.05	75.36±19.66	0.071±0.017
Md AC	1,185.02±129.98	215.22±47.66	0.182±0.035	1,237.07±88.46	195.84±43.94	0.158±0.033
E	1,739.25±217.47	88.36±29.67	0.050±0.015	1,739.51±217.45	88.43±29.71	0.050±0.015

Data are presented as mean±standard deviation for each parameter from 43 patient images

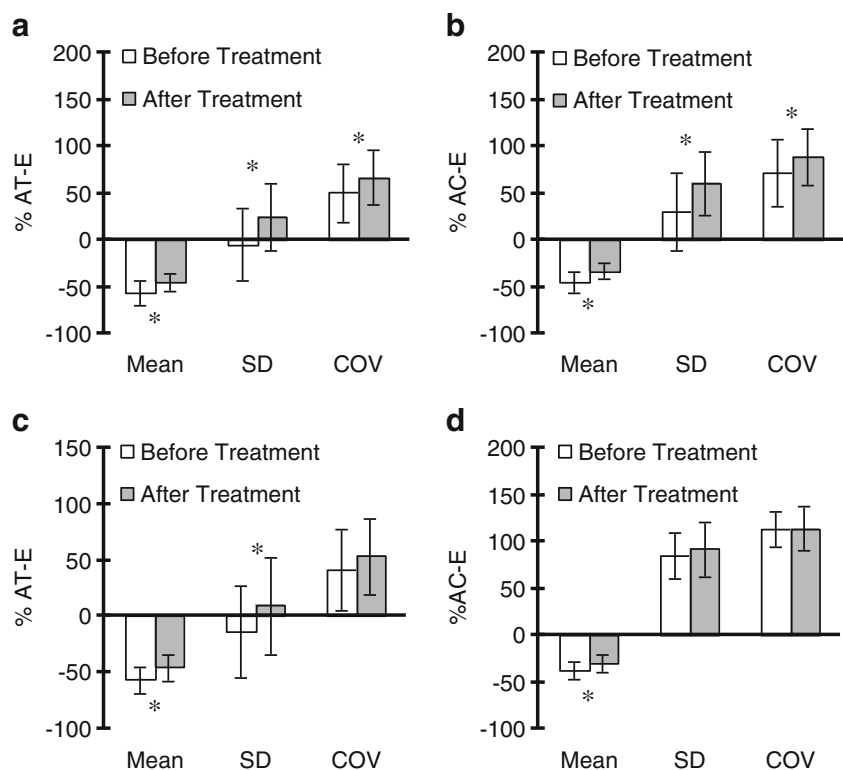
Discussion

All of the CT attenuation parameters (mean and variability (SD and COV)) of the AC region had higher values than those of the AT region independent of location (Mx and Md) and treatment status. The COV of AT and the mean of AC are the CT attenuation parameters that altered the regional variation between the Mx and Md after orthodontic treatment. The percentage (%) difference of variability of CT attenuation values changed for both the AT and AC in the Mx after orthodontic treatment, while that changed for only the AT in the Md. The CT attenuation value is equivalent to the DBM of which the distribution results from bone remodeling. Taken together, the current results indicated that active bone biological activities during orthodontic treatment

changed the distribution of alveolar bone mineralization differently between the maxilla and mandible. The current results also suggested that the clinical CBCT-based DBM analysis could be used to detect alterations resulting from active remodeling due to jaw bone complication.

Many studies indicated that CBCT can be used to assess bone mineral density as reliably as well-established methods including MSCT, dual-energy X-ray absorptiometry, and micro-CT in vitro and in vivo [28, 33–35]. It was found that CBCT-based density analysis is applicable to examine orthodontic cases [15, 16]. However, it was also indicated that different scanning conditions could alter CBCT attenuation value-based measures of bone mineral density [29, 30, 36–38]. The CBCT attenuation value may be inconsistent even when taken from the same patient at different times. In

Fig. 2 Comparison between before and after orthodontic treatment for the percentage (%) differences of the CT attenuation parameters (mean, SD, and COV) between the alveolar trabecular and cortical regions (AT and AC) and enamel (E) in the maxilla (**a, b**) and in the mandible (**c, d**). The error bars represent the standard deviation of each parameter. Asterisk denotes $p < 0.05$



the current study, we compared the absolute CBCT attenuation values between oral regions in the same image, while the percentage difference relative to the internal reference was used to compare the changes of CT attenuation value between the different CBCT images obtained before and after orthodontic treatment. This approach could reveal the significant regional variations of CT attenuation parameters at the same time and identify the oral bone locations that were substantially changed at the different time points during orthodontic treatment.

Appropriate internal references are needed to obtain comparable percentage differences of CT attenuation values between different CBCT images. As the enamel is acellular and avascular [39], it has no remodeling activity and is not affected by growth. As such, its mineral density is relatively stable and can serve as a good reference to measure bone mineral contents as suggested in previous studies. We chose the enamel region on the lingual side of the mandibular left second premolar since this area was not subject to the risk of demineralization by the etching procedure during bracket bonding and has the lowest risk of developing carious lesion that would affect its mineralization status [40]. The lingual cusp of this tooth is less likely to have attrition since it is a non-functional cusp and can be used as a reliable landmark to locate the same region.

It was observed that the active bone remodeling decreases the mean of DBM while increasing the variability of DBM (SD and COV) [41–43]. It was also found that the mean and variability of DBM has positive relationships with modulus and strength and viscoelastic property of the bone [19, 20]. In the case of orthodontic treatment, the applied orthodontic force stimulates alveolar bone remodeling resulting in alteration of DBM distribution, which in turn affects the degree of stimulus from the applied force. Combined together, these findings suggested that assessment of DBM distribution is of importance in understanding the progress of the alveolar bone remodeling and in estimating its mechanical response to the applied orthodontic force.

We found that the alveolar cortical region had higher values of all CT attenuation parameters than the alveolar trabecular region. The whole range of CT attenuation values in the AT region overlaps the range of lower CT attenuation values in the AC region. Simultaneously, AC is also composed of local regions with higher CT attenuation values than AT. As such, the mean and SD values were higher in AC than those in AT. It is generally accepted that cortical bone has higher tissue mineral density than trabecular bone. Furthermore, the larger surface area of trabecular bone provides more chance to recruit bone cells for remodeling resulting in more new (less mineralized) tissue area [44]. Thus, the wider distribution of the CT attenuation values in AC may arise from the combination of higher mineralization at the inner region of the cortical bone with less bone

remodeling activity and less mineral contents at the surface region.

The higher variability of CT attenuation values of the alveolar cortical region in the mandible than those in the maxilla may indicate that the mandibular cortical region of human patients was more remodeled than the maxillary cortical region. This regional variation is consistent with previous histomorphological studies on bone remodeling patterns in the jaw bones of dogs [45–47]. Earlier animal studies showed that the mandible was under torsion forces during functional masticatory movements [48–50], which may cause higher bone remodeling rate in the mandible. The regional variation of CT attenuation values in oral bone observed in the current study indirectly reveals that bone remodeling in human is different at local oral regions reflecting its functional demand.

The longitudinal comparison of the percentage differences of CT attenuation parameters before and after orthodontic treatment provided more information to understand how the DBM distribution is altered by orthodontic treatment. Maxillary alveolar region seems to be substantially changed by orthodontic treatment because all of the percentage differences of the mean and variability (SD and COV) between the enamel and alveolar regions increased. On the other hand, only mean of the percentage difference increased significantly in the mandibular alveolar cortical region while both mean and variability (SD) increased in the mandibular alveolar trabecular region. This result may indicate that bone remodeling at the alveolar cortical region in the mandible was not stimulated by orthodontic treatment up to the comparable level of other regions. This clinical CBCT-based DBM analysis may help provide more useful information for the clinical practice. For instance, the less activities of bone remodeling may increase the risk of relapse in this region after orthodontic treatment. Further post-treatment studies are demanded to evaluate such a relationship between DBM distribution changes and post-treatment stability.

The different responses to orthodontic tooth movement between the human maxillary and mandibular alveolar cortical bones observed in this study may be attributed to structural and biomechanical factors. It was demonstrated that at a sufficient level, orthodontic force can bend the alveolar process mechanically [51]. Under the same load level, the deformation, or strain, was greater in the mechanically weaker part of the bone [52]. In human, the maxilla has thinner cortical bone compared with the mandible as observed before [53, 54], so strain will be greater in the maxillary than in the mandible alveolar cortical bone under similar mechanical load. The higher strains in the bone lead to more microcrack and diffuse microdamage formation [55, 56], which have been found to be induced by orthodontic tooth movement with significantly higher density in the buccal cortical bones [57]. Microcracks and microdamages

are potent factors triggering bone remodeling [58]; therefore, it is highly likely that the higher activation of bone remodeling by orthodontic treatment in the maxillary than in the mandibular alveolar cortical bone is due to higher strain causing more microcracks and microdamages in the maxilla. The active bone remodeling during orthodontic treatment removes the damaged pre-existing old bone tissue that is replaced with new bone tissue. As a result, the variability of bone density increases. Our finding that the variability of DBM changed in the alveolar process after orthodontic treatment likely reflects the active biological activities of bone turnover.

The limitation of the current study was that a global segmentation value for each CBCT image was utilized to distinguish bone and non-bone voxels. Although this global segmentation is the most widely used method, the coarse process of segmentation and related partial volume effect would limit the accuracy of DBM values for bone voxels next to non-bone voxels. Partial volume effect artifact is another concern. With relative large voxel sizes of CBCT used in this study, the density values may not be strictly precise. It has been indicated that the partial volume effect is an inherent artifact when the CT attenuation values are averaged at the border line between different materials because the cubic voxels of CT image are not able to accurately delineate the shape of the irregular border line. Smaller voxel size (higher resolution) images may reduce these inherent errors of CBCT image analysis. However, increasing image resolution requires increasing radiation dose to patients, which is not in accordance with the “as low as reasonably achievable” principle. The segmentation algorithm used in this study provides a more conservative global threshold value than other algorithms, which can isolate the voxels with apparently higher CT values compared to neighbor voxels [32]. Although the voxels with lower CT value at the border line between the bone and soft tissue may be lost using this global segmentation, it may be helpful to reduce the partial volume effect on investigation of the CT attenuation distribution in the whole bone. While the segmentation methods and CT scanners currently utilized in clinic are still limited, the significant results for the regional variations of absolute CT attenuation values in the same image and the relative percentage difference changes between images indicate that current CBCT analysis method may be a legitimate solution to minimize the errors associated with CT attenuation value analysis. This study lacked a group which did not receive orthodontic treatment as an external control to assure that the findings in the treated group did not result from systematic bone remodeling in a patient during CBCT recording period. Histomorphological analyses in previous animal studies showed that the level of alveolar bone remodeling was not affected by normal growth [45–47]. Although these studies used a canine

model, those histomorphological results provided a direct evidence for the independence of jaw bone remodeling process from a systematic bone remodeling process in association with growth. In this study, we assumed the CT attenuation values in the CBCT images taken before orthodontic treatment as the control baseline from which the CT attenuation values changed during orthodontic treatment. Thus, the scope of this study was limited only for the orthodontic treatment cases.

Conclusions

This study used a relatively large sample of live human patients' CBCT images to assess changes of bone mineral distribution in the human maxillary and mandibular alveolar processes after orthodontic treatment. We identified that the alveolar cortical region of the mandible responded to orthodontic treatment differently compared with other alveolar regions. The new approach introduced in this study for non-invasive clinical CBCT image-based bone mineralization analysis could provide more practical information to understand the progress of orthodontic treatment in human patients.

Acknowledgments We thank the Delta Dental Foundation for providing financial support for this research through the Dental Master's Thesis Award Program. We thank the Orthodontic Department at Case Western Reserve University for providing us with the CBCT images used in this study.

Conflict of interest The authors declare that they have no conflict of interest.

References

1. Redlich M, Shoshan S, Palmon A (1999) Gingival response to orthodontic force. *Am J Orthod Dentofacial Orthop* 116:152–158
2. Baumrind S (1969) A reconsideration of the propriety of the “pressure-tension” hypothesis. *Am J Orthod* 55:12–22
3. Engstrom C, Granstrom G, Thilander B (1988) Effect of orthodontic force on periodontal tissue metabolism. A histologic and biochemical study in normal and hypocalcemic young rats. *Am J Orthod Dentofacial Orthop* 93:486–495
4. Miyoshi K, Igarashi K, Saeki S, Shinoda H, Mitani H (2001) Tooth movement and changes in periodontal tissue in response to orthodontic force in rats vary depending on the time of day the force is applied. *Eur J Orthodont* 23:329–338
5. Krishnan V, Davidovitch Z (2006) Cellular, molecular, and tissue-level reactions to orthodontic force. *Am J Orthod Dentofacial Orthop* 129:469.e1–e32. doi:10.1016/j.ajodo.2005.10.007
6. Rygh P (1973) Ultrastructural changes in pressure zones of human periodontium incident to orthodontic tooth movement. *Acta Odontol Scand* 31:109–122
7. Rygh P (1973) Ultrastructural changes of the periodontal fibers and their attachment in rat molar periodontium incident to orthodontic tooth movement. *Scand J Dent Res* 81:467–480

8. Grimm FM (1972) Bone bending, a feature of orthodontic tooth movement. *Am J Orthod* 62:384–393
9. Katona TR, Paydar NH, Akay HU, Roberts WE (1995) Stress analysis of bone modeling response to rat molar orthodontics. *J Biomech* 28:27–38
10. Keeling SD, King GJ, McCoy EA, Valdez M (1993) Serum and alveolar bone phosphatase changes reflect bone turnover during orthodontic tooth movement. *Am J Orthod Dentofacial Orthop* 103:320–326
11. Lilja E, Lindskog S, Hammarstrom L (1984) Alkaline phosphatase activity and tetracycline incorporation during initial orthodontic tooth movement in rats. *Acta Odontol Scand* 42:1–11
12. King GJ, Keeling SD, Wronski TJ (1991) Histomorphometric study of alveolar bone turnover in orthodontic tooth movement. *Bone* 12:401–409
13. Melsen B (1999) Biological reaction of alveolar bone to orthodontic tooth movement. *Angle Orthod* 69:151–158. doi:10.1043/0003-3219(1999)069<0151:BROABT>2.3.CO;2
14. Deguchi T, Takano-Yamamoto T, Yabuuchi T, Ando R, Roberts WE, Garetto LP (2008) Histomorphometric evaluation of alveolar bone turnover between the maxilla and the mandible during experimental tooth movement in dogs. *Am J Orthod Dentofacial Orthop* 133:889–897
15. Hsu J-T, Chang H-W, Huang H-L, Yu J-H, Li Y-F, Tu M-G (2010) Bone density changes around teeth during orthodontic treatment. *Clin Oral Investig* 15:511–519. doi:10.1007/s00784-010-0410-1
16. Chang HW, Huang HL, Yu JH, Hsu JT, Li YF, Wu YF (2012) Effects of orthodontic tooth movement on alveolar bone density. *Clin Oral Investig* 16:679–688. doi:10.1007/s00784-011-0552-9
17. Roschger P, Fratzl P, Eschberger J, Klaushofer K (1998) Validation of quantitative backscattered electron imaging for the measurement of mineral density distribution in human bone biopsies. *Bone* 23:319–326
18. Ruffoni D, Fratzl P, Roschger P, Klaushofer K, Weinkamer R (2007) The bone mineralization density distribution as a fingerprint of the mineralization process. *Bone* 40:1308–1319
19. Follet H, Boivin G, Rumelhart C, Meunier PJ (2004) The degree of mineralization is a determinant of bone strength: a study on human calcanei. *Bone* 34:783–789
20. Kim DG, Shertok D, Ching Tee B, Yeni YN (2011) Variability of tissue mineral density can determine physiological creep of human vertebral cancellous bone. *J Biomech* 44:1660–1665. doi:10.1016/j.jbiomech.2011.03.025
21. Verna C, Zaffe D, Siciliani G (1999) Histomorphometric study of bone reactions during orthodontic tooth movement in rats. *Bone* 24:371–379
22. Scarfe WC, Farman AG, Sukovic P (2006) Clinical applications of cone-beam computed tomography in dental practice. *J Can Dent Assoc* 72:75–80
23. Hilgers ML, Scarfe WC, Scheetz JP, Farman AG (2005) Accuracy of linear temporomandibular joint measurements with cone beam computed tomography and digital cephalometric radiography. *Am J Orthod Dentofacial Orthop* 128:803–811. doi:10.1016/j.ajodo.2005.08.034
24. Scarfe WC, Farman AG (2008) What is cone-beam CT and how does it work? *Dent Clin North Am* 52:707–730. doi:10.1016/j.cden.2008.05.005
25. Roberts JA, Drage NA, Davies J, Thomas DW (2009) Effective dose from cone beam CT examinations in dentistry. *Br J Radiol* 82:35–40. doi:10.1259/bjr/31419627
26. Ludlow JB, Davies-Ludlow LE, Brooks SL (2003) Dosimetry of two extraoral direct digital imaging devices: NewTom cone beam CT and orthophos plus DS panoramic unit. *Dentomaxillofac Radiol* 32:229–234
27. Naitoh M, Katsumata A, Mitsuya S, Kamemoto H, Arijii E (2004) Measurement of mandibles with microfocus x-ray computerized tomography and compact computerized tomography for dental use. *Int J Oral Maxillofac Implants* 19:239–246
28. Nomura Y, Watanabe H, Honda E, Kurabayashi T (2010) Reliability of voxel values from cone-beam computed tomography for dental use in evaluating bone mineral density. *Clin Oral Implants Res* 21:558–562. doi:10.1111/j.1600-0501.2009.01896.x
29. Kwong JC, Palomo JM, Landers MA, Figueroa A, Hans MG (2008) Image quality produced by different cone-beam computed tomography settings. *Am J Orthod Dentofacial Orthop* 133:317–327. doi:10.1016/j.ajodo.2007.02.053
30. Loubele M, Jacobs R, Maes F, Denis K, White S, Coudyzer W, Lambrechts I, van Steenberghe D, Suetens P (2008) Image quality vs radiation dose of four cone beam computed tomography scanners. *Dentomaxillofac Radiol* 37:309–318. doi:10.1259/dmfr/16770531
31. Verna C, Dalstra M, Melsen B (2000) The rate and the type of orthodontic tooth movement is influenced by bone turnover in a rat model. *Eur J Orthod* 22:343–352
32. Kuhn JL, Goldstein SA, Feldkamp LA, Goulet RW, Jesion G (1990) Evaluation of a microcomputed tomography system to study trabecular bone structure. *J Orthop Res* 8:833–842. doi:10.1002/jor.1100080608
33. Naitoh M, Hirukawa A, Katsumata A, Arijii E (2009) Evaluation of voxel values in mandibular cancellous bone: relationship between cone-beam computed tomography and multislice helical computed tomography. *Clin Oral Implants Res* 20:503–506. doi:10.1111/j.1600-0501.2008.01672.x
34. González-García R, Monje F (2011) The reliability of cone-beam computed tomography to assess bone density at dental implant recipient sites: a histomorphometric analysis by micro-CT. *Clin Oral Implants Res*. doi:10.1111/j.1600-0501.2011.02390.x
35. Marquezan M, Lau TC, Mattos CT, Cunha AC, Nojima LI, Sant'Anna EF, Souza MM, Araujo MT (2012) Bone mineral density. *Angle Orthod* 82:62–66. doi:10.2319/031811-192.1
36. Bryant JA, Drage NA, Richmond S (2008) Study of the scan uniformity from an i-CAT cone beam computed tomography dental imaging system. *Dentomaxillofac Radiol* 37:365–374. doi:10.1259/dmfr/13227258
37. Nackaerts O, Maes F, Yan H, Couto Souza P, Pauwels R, Jacobs R (2011) Analysis of intensity variability in multislice and cone beam computed tomography. *Clin Oral Implants Res* 22:873–879. doi:10.1111/j.1600-0501.2010.02076.x
38. Katsumata A, Hirukawa A, Okumura S, Naitoh M, Fujishita M, Arijii E, Langlais RP (2007) Effects of image artifacts on gray-value density in limited-volume cone-beam computerized tomography. *Oral Surg Oral Med Oral Pathol Oral Radiol Endod* 104:829–836. doi:10.1016/j.tripleo.2006.12.005
39. Smith CE (1998) Cellular and chemical events during enamel maturation. *Crit Rev Oral Biol Med* 9:128–161
40. Demirci M, Tuncer S, Yucookur AA (2010) Prevalence of caries on individual tooth surfaces and its distribution by age and gender in university clinic patients. *Eur J Dent* 4:270–279
41. Yao W, Cheng Z, Koester KJ, Ager JW, Balooch M, Pham A, Chefo S, Busse C, Ritchie RO, Lane NE (2007) The degree of bone mineralization is maintained with single intravenous bisphosphonates in aged estrogen-deficient rats and is a strong predictor of bone strength. *Bone* 41:804–812
42. Busse B, Hahn M, Soltan M, Zustin J, Puschel K, Duda GN, Amling M (2009) Increased calcium content and inhomogeneity of mineralization render bone toughness in osteoporosis: mineralization, morphology and biomechanics of human single trabeculae. *Bone* 45:1034–1043. doi:10.1016/j.bone.2009.08.002
43. Ames MS, Hong S, Lee HR, Fields HW, Johnston WM, Kim DG (2010) Estrogen deficiency increases variability of tissue mineral density of alveolar bone surrounding teeth. *Arch Oral Biol* 55:599–605. doi:10.1016/j.archoralbio.2010.05.011

44. Allen MR, Turek JJ, Phipps RJ, Burr DB (2011) Greater magnitude of turnover suppression occurs earlier after treatment initiation with risedronate than alendronate. *Bone* 49:128–132. doi:10.1016/j.bone.2010.07.011
45. Huja SS, Fernandez SA, Hill KJ, Li Y (2006) Remodeling dynamics in the alveolar process in skeletally mature dogs. *Anat Rec Part A* 288A:1243–1249
46. Huja SS, Beck FM (2008) Bone remodeling in maxilla, mandible, and femur of young dogs. *Anatomical Record (Hoboken, NJ: 2007)* 291:1–5
47. Randall LE, Beck FM, Huja SS (2011) Bone remodeling surrounding primary teeth in skeletally immature dogs. *Angle Orthod* 81:931–937. doi:10.2319/021611-114.1
48. Hylander WL, Crompton AW (1986) Jaw movements and patterns of mandibular bone strain during mastication in the monkey *Macaca fascicularis*. *Arch Oral Biol* 31:841–848
49. Daegling DJ, Hylander WL (2000) Experimental observation, theoretical models, and biomechanical inference in the study of mandibular form. *Am J Phys Anthropol* 112:541–551
50. Ravosa MJ, Johnson KR, Hylander WL (2000) Strain in the galago facial skull. *J Morphol* 245:51–66. doi:10.1002/1097-4687(200007)245:1<51::AID-JMOR4>3.0.CO;2-7
51. Meikle MC (2006) The tissue, cellular, and molecular regulation of orthodontic tooth movement: 100 years after Carl Sandstedt. *Eur J Orthod* 28:221–240. doi:10.1093/ejo/cjl001
52. Fyhrie DP, Vashishth D (2000) Bone stiffness predicts strength similarly for human vertebral cancellous bone in compression and for cortical bone in tension. *Bone* 26:169–173. doi:10.1016/s8756-3282(99)00246-x
53. Roberts WE, Arbuckle GR, Analoui M (1996) Rate of mesial translation of mandibular molars using implant-anchored mechanics. *Angle Orthod* 66:331–338. doi:10.1043/0003-3219(1996)066<0331:ROMTOM>2.3.CO;2
54. Roberts WE (2005) Bone physiology, metabolism, and biomechanics in orthodontic practice. In: Graber TM, Vanarsdall RL, Vig KWL (eds) *Orthodontics: current principles and techniques*. Mosby, St. Louis, pp 221–292
55. Boyce TM, Fyhrie DP, Glotkowski MC, Radin EL, Schaffler MB (1998) Damage type and strain mode associations in human compact bone bending fatigue. *J Orthop Res* 16:322–329. doi:10.1002/jor.1100160308
56. Reilly GC, Currey JD (1999) The development of microcracking and failure in bone depends on the loading mode to which it is adapted. *J Exp Biol* 202:543–552
57. Verna C, Dalstra M, Lee TC, Cattaneo PM, Melsen B (2004) Microcracks in the alveolar bone following orthodontic tooth movement: a morphological and morphometric study. *Eur J Orthod* 26:459–467
58. Burr DB, Martin RB, Schaffler MB, Radin EL (1985) Bone remodeling in response to in vivo fatigue microdamage. *J Biomech* 18:189–200

Copyright of Clinical Oral Investigations is the property of Springer Science & Business Media B.V. and its content may not be copied or emailed to multiple sites or posted to a listserv without the copyright holder's express written permission. However, users may print, download, or email articles for individual use.